14th International Conference on Applications of Statistics and Probability in Civil Engineering, ICASP14
Dublin, Ireland, July 9-13, 2023

Bridge abnormality detection utilizing acceleration of a moving vehicle

Soichiro Hasegawa
Ph.D. Candidate, Dept. of Civil and Earth Resources Engineering, Kyoto University - Kyoto, Japan.

Chul-Woo Kim
Professor, Dept. of Civil and Earth Resources Engineering, Kyoto University - Kyoto, Japan.

Kai-Chun Chang
Junior Assc. Professor, Dept. of Civil and Earth Resources Engineering, Kyoto University - Kyoto, Japan.

Yi Zhang
Assc. Professor, Tsinghua University, Beijing, China

ABSTRACT: This study aims to propose a bridge anomaly detection method utilizing measured vehicle accelerations. The proposed method can determine the existence of any anomaly utilizing the difference between the measured vehicle accelerations at the inspection phase and the reference acceleration when the bridge is considered healthy. The bandpass filter (BPF) is applied to the accelerations before the subtraction to eliminate any undesirable vibration components other than the vibration derived from the bridge. The advantage of the proposed method is (1) no information on the vehicle properties is needed as input, (2) the method is theoretically simple and easy to understand, and (3) by calculating a damage indicator value using multiple measured data, it is possible to estimate the level of damage as well as the reliability of the results. The feasibility of the proposed method is investigated by a laboratory experiment using a model vehicle equipped with accelerometers. Observations showed that the method successfully classifies the bridge damage conditions with acceptable accuracy.

1. INTRODUCTION

In the field of bridge health monitoring (BHM), a number of studies have been conducted. The most basic method is to detect anomalies by determining changes in the bridge modal parameters based on the measurements from sensors directly attached to the bridge (Salawu 1997; Carden and Fanning 2004). Although these direct-measurement methods are relatively accurate, they are labor- and time-consuming. To cope with this problem, the drive-by BHM which inspects bridge health conditions utilizing measured data on the test vehicles have been investigated (e.g., Yang and Chang 2009; Kim and Kawatani 2009; O'Brien et al. 2014).

Drive-by BHM is advantageous in terms of efficiency, but the challenge is to achieve sufficient accuracy for practical use. Many drive-by BHM methods of identifying the modal parameters of a bridge are proposed. One of the most basic concepts of the drive-by BHM methods is to extract the bridge's natural frequencies from accelerations measured on the test vehicles (e.g., Yang and Chang 2009). Mode shape and damping are also focused on as damage-sensitive features of the drive-by BHM in several studies (e.g., González et al. 2012).

Apart from these modal parameters-based methods, the anomaly detection method utilizing a damage indicator estimated using the measured vehicle vibrations is also proposed. As individual modal parameters of bridges may not be sensitive

enough to detect bridge damage, there is a strong need to develop damage-sensitive features other than modal parameters. For example, the wavelet-based approach is one of the effective methods (Fitzgerald et al. 2019), and Zhang et.al (2022) validated its effectivity through a laboratory experiment.

For the practical application and dissemination of the drive-by BHM method, it is crucial to be simple and easy to understand. Therefore, in this study, a simple non-modal parameter-based method for detecting bridge anomalies using measured vehicle responses is proposed. In the proposed method, vehicle accelerations are measured both when the bridge is healthy and when the bridge is suspected to be damaged. A band-pass filter (BPF) is applied to both measured accelerations with a passband around the natural frequency of the first bending mode of the target bridge. The difference between the two accelerations is then calculated in the time domain to check the amplitude of the difference. If the amplitude is greater than a threshold value, it can be concluded that the bridge is likely to be damaged. The feasibility of the proposed method was investigated through laboratory experiments using a scaled model vehicle and a bridge.

Another method is to use the PSD of acceleration or the contact point displacement (CP) estimated by the vehicle acceleration as an input signal, rather than the vehicle acceleration. Therefore, the accuracies of those three different inputs are also investigated. Here, the CP displacement denotes a vertical displacement at the contact point between a vehicle tire and the road surface along the vehicle traveling direction, which is the sum of the road surface profile and bridge vibration displacement.

2. ANOMALY DETECTION SCHEME

The procedure for damage detection using the time history of the vehicle accelerations is summarized as follows.

Preliminary step
1. The vehicle accelerations while running through the target bridge are measured for N times.
2. The BPF around the natural frequency of the 1st bending mode of the bridge is applied to the accelerations.
3. The average of the bandpass filtered acceleration of the N times measurements is calculated. It is named reference acceleration.

Test step
1. The vehicle accelerations while running through the target bridge are measured for N times.
2. The BPF around the natural frequency of the 1st bending mode of the bridge is applied to the accelerations.
3. Estimate differences between filtered test accelerations and reference acceleration.
4. The root mean squares (RMS) values of the differences are calculated.
5. The likelihood of bridge damage being present is statistically examined using RMS values.

The procedure for damage detection using the PSDs of the vehicle accelerations is summarized as follows.

Preliminary step
1. The vehicle accelerations while running through the target bridge are measured for N times.
2. The BPF around the natural frequency of the 1st bending mode of the bridge is applied to the accelerations.
3. Each of the filtered accelerations is converted to the PSDs.
4. The average PSD of the N times measurements is calculated. It is named reference PSD.

Test step
1. The vehicle accelerations while running through the target bridge are measured for N times.
2. The BPF around the natural frequency of the 1st bending mode of the bridge is applied to the accelerations.
3. Each of the filtered accelerations is converted to the PSDs.
4. Estimate the difference between the PSDs of the test accelerations and the reference PSD.
5. The RMS values are calculated for each difference of the PSDs in a predefined

frequency range around the natural frequency of the 1st bending mode of the bridge.
6. The likelihood of bridge damage being present is statistically examined using RMS values.

The procedure for damage detection using the estimated contact-point (CP) displacements is summarized as follows.

Preliminary step
1. The vehicle accelerations while running through the target bridge are measured for N times.
2. The CP displacements are estimated by each of the measured accelerations after the lowpass filter (LPF) is applied to eliminate noises.
3. The BPF around the natural frequency of the 1st bending mode of the bridge is applied to the estimated CP displacements.
4. The average CP displacement of the N times measurements is calculated. It is named reference CP displacement.

Test step
1. The vehicle accelerations while running through the target bridge are measured for N times.
2. The CP displacements are estimated by each of the measured accelerations after the LPF is applied to eliminate noises.
3. The BPF around the natural frequency of the 1st bending mode of the bridge is applied to the estimated CP displacements.
4. Estimate the difference between CP displacements estimated from the test accelerations and the reference CP displacement.
5. The RMS values are calculated for each difference in CP displacements.
6. The likelihood of bridge damage being present is statistically examined using RMS values.

3. CP DISPLACEMENT IDENTIFICATION METHOD

The CP displacement (Yang et al. 2018) identification method which solves a regularized least square minimization with a dynamic programming technique is introduced in this chapter. This method (Hasegawa et al. 2023) is an improved method of the CP displacement identification method utilizing a moving force identification (MFI) algorithm (McGetrick et al. 2013).

A vehicle model is a two-degree-of-freedom half-car model shown in Figure 1. An equation of motion of the vehicle is written as Eq. (1).

$$\boldsymbol{M}_v\ddot{\boldsymbol{y}}_v + \boldsymbol{C}_v\dot{\boldsymbol{y}}_v + \boldsymbol{K}_v\boldsymbol{y}_v = \boldsymbol{f}_v \tag{1}$$

where, $\boldsymbol{M}_v$, $\boldsymbol{C}_v$, and $\boldsymbol{K}_v$ denote mass, damping, and stiffness matrices of the vehicle, respectively. $\boldsymbol{y}_v$ denotes a displacement vector of the vehicle. The dots above the variables represent derivatives in the time domain. $\boldsymbol{f}_v$ denotes a dynamic vehicle force vector calculated by Eq. (2).

$$\boldsymbol{f}_v = \boldsymbol{K}_r\boldsymbol{r} + \boldsymbol{C}_r\dot{\boldsymbol{r}} \tag{2}$$

where $\boldsymbol{r}(=\{r_1, r_2\}^T)$ denotes a CP displacement vector along the passage under the vehicle tires. r_1 and r_2 denote the profiles under the front and rear tires, respectively. When the vehicle travels on bridges the profile comprises both road surface roughness and bridge deflection. $\boldsymbol{K}_r$ and $\boldsymbol{C}_r$ are calculated as Eq. (3) and Eq. (4), respectively.

$$\boldsymbol{K}_r = \begin{bmatrix} K_1 & K_2 \\ D_1K_1 & -D_2K_2 \end{bmatrix} \tag{3}$$

$$\boldsymbol{C}_r = \begin{bmatrix} C_1 & C_2 \\ D_1C_1 & -D_2C_2 \end{bmatrix} \tag{4}$$

where C_i, K_i, and D_i denote the suspension stiffness, suspension damping and horizontal distance from the i-th axle to the centroid of the vehicle, respectively. $i = 1, 2$ indicate the front and rear axle, respectively. Eq. (1) can be rewritten to a continuous-time state-space expression as Eq. (5).

$$\dot{\boldsymbol{X}} = \boldsymbol{A}\boldsymbol{X} + \boldsymbol{g} \tag{5}$$

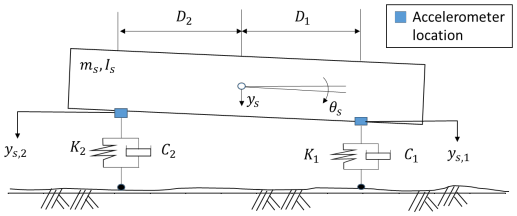

Figure 1: Two-degree-of-freedom half-car model.

where $\boldsymbol{X}$, $\boldsymbol{A}$, and $\boldsymbol{g}$ are defined as Eq. (6), Eq. (7) and Eq. (8).

$$\boldsymbol{X} = \begin{Bmatrix} \boldsymbol{y}_v \\ \dot{\boldsymbol{y}}_v \end{Bmatrix} \tag{6}$$

$$\boldsymbol{A} = \begin{bmatrix} \boldsymbol{0} & \boldsymbol{I} \\ -\boldsymbol{M}_v^{-1}\boldsymbol{K}_v & -\boldsymbol{M}_v^{-1}\boldsymbol{C}_v \end{bmatrix} \tag{7}$$

$$\boldsymbol{g} = \begin{bmatrix} \boldsymbol{0} \\ \boldsymbol{M}_v^{-1}\boldsymbol{f}_v \end{bmatrix} \tag{8}$$

By solving Eq. (5) as a first-order differential equation, a discrete-time state-space equation is obtained as Eq. (9).

$$\boldsymbol{X}_{j+1} = \boldsymbol{M}\boldsymbol{X}_j + \boldsymbol{G}\boldsymbol{f}_{v,j} \tag{9}$$

where $\boldsymbol{M}=e^{\boldsymbol{A}h}$ is the exponential matrix that can be calculated by the Pade approximation and h is the time step. $\boldsymbol{f}_{v,j}$ is the dynamic vehicle force vector at a time j, which contains the force in bounce and pitch directions. $\boldsymbol{G}$ is defined as Eq. (10).

$$\boldsymbol{G} = \boldsymbol{A}^{-1}(\boldsymbol{M} - \boldsymbol{I}) \begin{bmatrix} \boldsymbol{0} \\ \boldsymbol{M}_v^{-1} \end{bmatrix} \tag{10}$$

Relationship between the CP displacement vector and its first derivative is defined as Eq. (11).

$$\dot{\boldsymbol{r}}_j = (\boldsymbol{r}_{j+1} - \boldsymbol{r}_j)/\Delta t \tag{11}$$

where Δt is an interval of discrete time steps. Defining a new state vector as Eq. (12), a new discrete-time state-space model is obtained as Eq. (13).

$$\widehat{\boldsymbol{X}}_j = \begin{bmatrix} \boldsymbol{X}_j^T & \boldsymbol{r}_j^T & \boldsymbol{r}_{j+1}^T \end{bmatrix}^T \tag{12}$$

$$\widehat{\boldsymbol{X}}_{j+1} = \begin{bmatrix} \boldsymbol{M} & \boldsymbol{G}_1 & \boldsymbol{G}_2 \\ \boldsymbol{0} & \boldsymbol{0} & \boldsymbol{I} \\ \boldsymbol{0} & \boldsymbol{0} & \boldsymbol{0} \end{bmatrix} \widehat{\boldsymbol{X}}_j + \begin{bmatrix} \boldsymbol{0} \\ \boldsymbol{0} \\ \boldsymbol{I} \end{bmatrix} \boldsymbol{r}_{j+2} \tag{13}$$

where, $\boldsymbol{G}_1$ and $\boldsymbol{G}_2$ are defined as Eq. (14) and Eq. (15), respectively.

$$\boldsymbol{G}_1 = \boldsymbol{G}(\boldsymbol{K}_r - \boldsymbol{C}_r/\Delta t) \tag{14}$$

$$\boldsymbol{G}_2 = \boldsymbol{G}\,\boldsymbol{C}_r/\Delta t \tag{15}$$

The advantage of the discrete-time state-space model defined in Eq. (13) is that this form makes dynamic programming more easily applicable by using the CP displacement vector as an external input term. Defining the measured vehicle acceleration vector as $\boldsymbol{d}_j$, the relationship between the measured vehicle acceleration vector and the state vector can be written as Eq. (16) and Eq. (17).

$$\boldsymbol{d}_j = \boldsymbol{Q}_0 \widehat{\boldsymbol{X}}_j \tag{16}$$

$$\boldsymbol{Q}_0 = \boldsymbol{M}_v^{-1}[-\boldsymbol{K}_v \quad -\boldsymbol{C}_v \quad (\boldsymbol{K}_r - \boldsymbol{C}_r/\Delta t) \quad \boldsymbol{C}_r/\Delta t] \tag{17}$$

The CP displacement vector is estimated from Eq. (13) and Eq. (16) using the regularized least square minimization, as it is an ill-posed inverse problem in which the slight change in the measured data causes a large difference in the estimated results. To deal with the ill-posed problem and obtain a robust solution, Tikhonov regularization (Tikhonov and Arsenin 1977) is applied. The cost function (*CF*) applied with Tikhonov regularization is defined as Eq. (18).

$$CF = \sum_{j=1}^{N} \left(\boldsymbol{d}_j - \boldsymbol{Q}_0 \widehat{\boldsymbol{X}}_j\right)^T \left(\boldsymbol{d}_j - \boldsymbol{Q}_0 \widehat{\boldsymbol{X}}_j\right) + \lambda \boldsymbol{r}_j^T \boldsymbol{r}_j \tag{18}$$

where N is the number of total time steps. λ stands for a regularization parameter that takes a balance between the volumes of the first and second terms in Eq. (18). The optimal value of λ can be obtained by L-curve method (Hansen and O'Leary 1993). In the L-curve method, candidate λ values need to be preset. For each candidate λ, the regularized least square minimization problem is solved and the L2 norm of error (E_{norm}) and L2 norm of the unknown parameter (F_{norm}) are obtained as Eq. (19) and Eq. (20), respectively.

$$E_{norm} = \sqrt{\sum_{j=1}^{N} \left(\boldsymbol{d}_j - \boldsymbol{Q}_0 \widehat{\boldsymbol{X}}_j\right)^T \left(\boldsymbol{d}_j - \boldsymbol{Q}_0 \widehat{\boldsymbol{X}}_j\right)} \tag{19}$$

$$F_{norm} = \sqrt{\sum_{j=1}^{N} \boldsymbol{r}_j^T \boldsymbol{r}_j} \tag{20}$$

E_{norm} and F_{norm} corresponding to the each of candidate λs is plotted on a log-log scale, where E_{norm} is placed on the horizontal axis and F_{norm}

Figure 2: Model bridge in experiment.

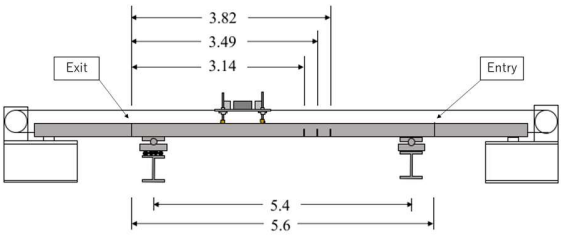

Figure 3: Model bridge dimensions.

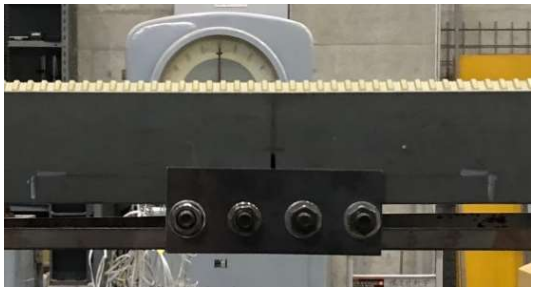

Figure 4: Slits reinforcement of bridge.

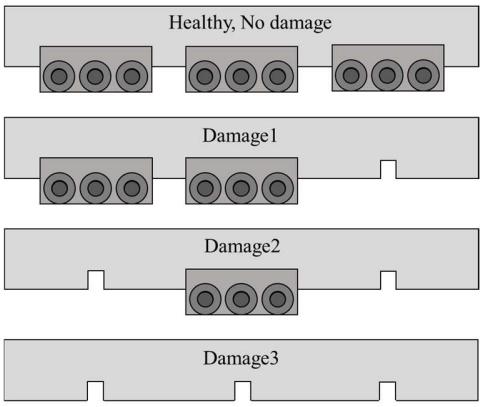

Figure 5: Damage cases in experiment.

is on the vertical axis. The point which has a maximum curvature is extracted as an optimal λ point.

4. VALIDATION BY LABORATORY EXPERIMENT

4.1. Experimental condition

To investigate the feasibility of the proposed damage detection method, a laboratory experiment using a model vehicle and bridge was conducted. The model bridge in the laboratory experiment is shown in Figure 2, which has a span length of 5.4 m and is a simply-supported steel bridge. Three slits at 3.14 m, 3.49 m, and 3.82 m from the exit were applied to reduce the flexural rigidity of the bridge as shown in Figure 3. These slits can be reinforced with a steel plate as shown in Figure 4. The state that all slits are reinforced is named “No Damage”. The state that two of three slits are reinforced is named “Damage 1”, and the state that one of three slits are reinforced is named “Damage 2”. Finally, the state where all slits are open is named “Damage 3”. Figure 5 shows all damage scenarios examined in this study.

In the preliminary step, 10 acceleration measurements were taken for 'No Damage' only. Next, in the test step, 10 acceleration measurements were taken for each damage scenario. The properties of the model bridge are shown in Table 1. Figure 6 shows the scaled road surface roughness for the model bridge, which was produced by scaling down a road roughness profile of an existing bridge with a span length of 40 m.

The properties of the model vehicle are shown in Figure 7 and Table 2. The suspension stiffness and damping constant of the front and rear axles are obtained by free vibration tests. Two accelerometers are installed on the front and rear axles of the model vehicle, respectively. The bounce acceleration at the center of gravity of the vehicle body is calculated by the two measured accelerations and used as the input signal for bridge damage detection. For CP displacement estimation, the bounce and pitch accelerations which are calculated by the two measured accelerations are used as the input signals. The accelerometers are M-A550AC32x produced by SEIKO Epson Co. Ltd., and the sampling frequency of the measurements was 200Hz. The vehicle speed was 1.26m/s which is also scaled speed using the speed parameter.

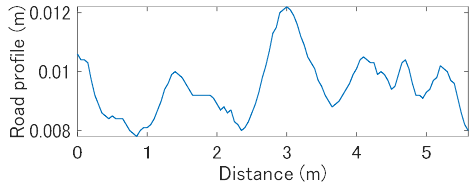

Figure 6: Road profile on the model bridge.

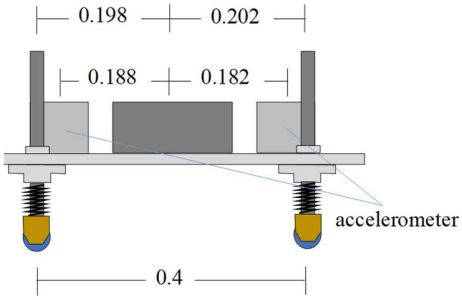

Figure 7: Model vehicle.

Table 1: Bridge model properties.

Property		Value
Span length		5.4 m
Mass per unit length		46.9 kg/m
Second moment of area		5.48×10^{-7}m^4
Young's modulus		2.1×10^{11} N/m^2
1st natural frequency	No damage	2.81 Hz
	Damage1	2.71 Hz
	Damage2	2.59 Hz
	Damage3	2.59 Hz

Table 2: Vehicle model properties.

Property		Value
Body mass		22.9 kg
Suspension stiffness	front	3480 N/m
	rear	3531 N/m
Suspension damping	front	3.51 N s/m
	rear	13.2 N s/m
Distance between front and rear axle		0.4 m
Natural frequency of bounce		2.83 Hz

4.2. Damage detection

For the damage detection, the BPF was applied before estimating the difference in the accelerations, and the cut-off frequency was set as 2.3Hz and 3.3Hz, considering the natural frequency of the 1st bending mode of the bridge. The cut-off frequency of the LPF applied to the accelerations before the CP displacement estimation is defined as 30Hz, considering the natural frequency of the 3rd bending mode of the bridge which was around 25Hz.

The averages of the difference of the acceleration, PSD, and CP displacements under the front and rear axles are shown in Figure 8, Figure 9, Figure 10 and Figure 11, respectively. In those figures, the higher the damage level is, the larger the amplitude of the difference becomes in all input signal types. This tendency is particularly noticeable when acceleration or PSD is used as the input signal. The same trend can be observed whether the input information is acceleration or PSD, but it is preferable to use acceleration as it does not require additional signal processing.

To evaluate the existence of bridge damage quantitatively, the Mahalanobis Distance (MD) of the RMS values is used as a damage indicator. MD is one of the distances which represents a statistical similarity among data groups, unlike the commonly used Euclidean distance.

In anomaly detection, the MD between the reference data group and newly obtained data is calculated. If the MD is greater than the threshold, a possible anomaly is indicated. Such anomaly detection utilizing MD is called Mahalanobis-Taguchi System (MTS) (Taguchi and Jugulum 2000). MD for the i-th data in the test case is calculated as Eq. (21) in the proposed method.

$$MD_i = \left| \frac{RMS_{test,i} - \mu_{ref}}{s_{ref}} \right| \tag{21}$$

where, $RMS_{test,i}$ denotes the RMS of the i-th acceleration difference in the test step. μ_{ref} and s_{ref} represent the mean and standard deviation of the RMS values of the difference of accelerations in the reference state. The difference of accelerations in the reference state is calculated using Eq.(22).

$$\boldsymbol{SUBACC}_{ref,i} = \boldsymbol{ACC}_{ref,i} - \frac{\sum_{j \neq i} \boldsymbol{ACC}_{ref,j}}{N-1} \tag{22}$$

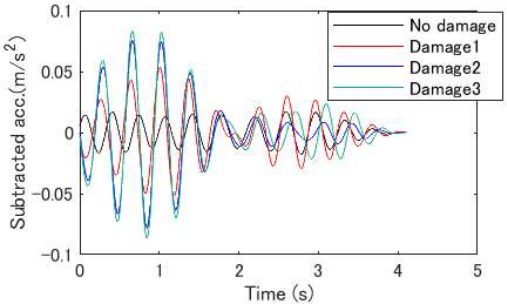

Figure 8: Difference in acceleration responses.

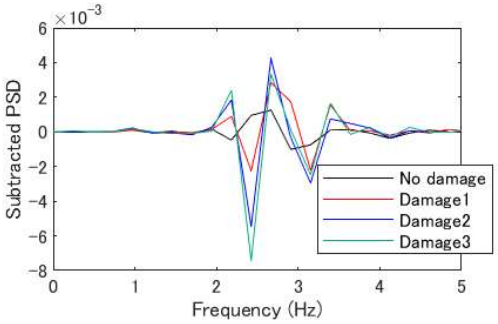

Figure 9: Difference in PSDs.

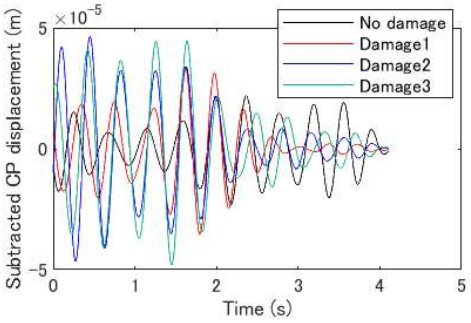

Figure 10: Difference in CP displacements at the front axle.

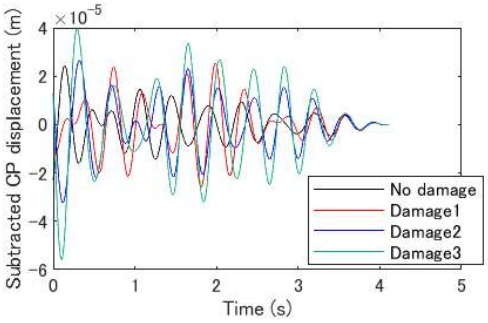

Figure 11: Difference in CP displacements at the rear axle.

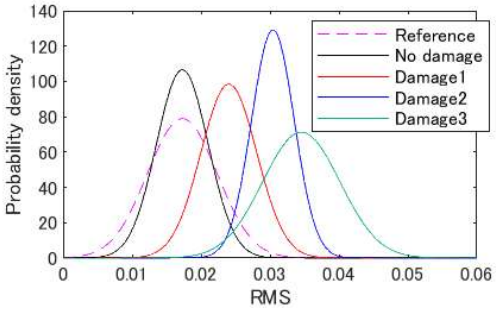

Figure 12: Normal distributions of RMS values in each damage level and reference RMS

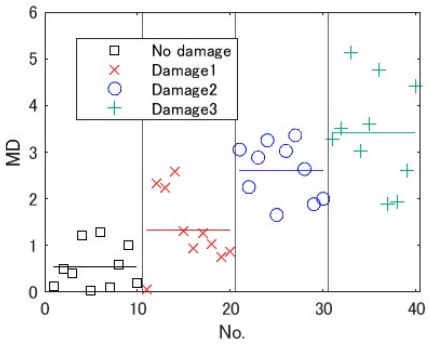

Figure 13: MDs calculated by RMS values in each damage level

where, $\boldsymbol{SUBACC}_{ref,i}$, and $\boldsymbol{ACC}_{ref,i}$ respectively denote the vector of difference of acceleration and acceleration vector in the reference state. Subscript i indicates i-th measured data in the preliminary step and N indicates the total number of measurements in the preliminary step.

Estimated RMS values of difference of accelerations in the reference and all test states can be fitted to the normal distribution as shown in Figure 12, which shows mean values of the ”reference” and ”No Damage” scenarios are similar, while the mean values of the damage scenarios differ from the reference state as damage severity increases. MD of the RMS values of the acceleration differences is shown in Figure 13. The mean values of MD increase according to an increase in damage severity, which indicates the effectiveness of MD as a damage indicator.

5. CONCLUSIONS

The feasibility of drive-by BHM using the difference of vehicle accelerations measured in the preliminary and test steps is investigated through laboratory experiments. Observations demonstrated that the greater the damage level, the greater the RMS value of the difference of the input signals, especially when accelerations or PSDs are used. By utilizing the MD of the RMS of the measured accelerations as a damage indicator, the possibility of the bridge damage was successfully scanned with possible damage levels.

ACKNOWLEDGMENTS

A part of this work is supported by JSPS Bilateral joint research projects, Grant No. JPJSBP120217405, which is greatly appreciated.

REFERENCES

Carden, E.P., and P. Fanning. (2004). "Vibration based condition monitoring: A review." *Structural Health Monitoring*, 3(4), 355–377.

Fitzgerald, P.C., Malekjafarian, A., Cantero, A., O'Brien, E.J., and Prendergast, L.J. (2019). "Drive-by scour monitoring of railway bridges using a wavelet-based approach." *Engineering Structures*, 191, 1–11.

González, A., O'Brien, E.J., and McGetrick, P.J. (2012). "Identification of damping in a bridge using a moving instrumented vehicle." *Journal of Sound and Vibration*, 331(18), 4115–4131.

Hansen, P.C., and O'Leary, D.P. (1993). "The Use of the L-Curve in the Regularization of Discrete Ill-Posed Problems." *SIAM Journal of Scientific Computing*, 14(6), 1487–1503.

Hasegawa, S., Kim, C.W., Toshi, N., and Chang, K.C. (2023) "Inverse Analysis for Road Roughness Profile Identification Utilizing Acceleration of a Moving Vehicle" *Experimental Vibration Analysis for Civil Engineering Structures*, 224, 643-651.

Kim, C.W., Isemoto, R., McGetrick, P.J., M. Kawatani, and O'Brien, E.J. (2014). "Drive-by bridge inspection from three different approaches." *Smart Structures and Systems*, 13(5), 775–796.

Kim, C.W., and Kawatani., M. (2009). "Challenge for a drive-by bridge inspection." *Safety, Reliability and Risk of Structures, Infrastructures and Engineering Systems,* 758–765.

McGetrick, P.J., Kim, C.W., González, A., and O'Brien, E.J. (2013). "Dynamic Axle Force and Road Profile Identification Using a Moving Vehicle." *International Journal of Architecture, Engineering and Construction*, 2(1), 1–16.

O'Brien, E.J., McGetrick, P.J., and González. A. (2014). "A drive-by inspection system via vehicle moving force identification." *Smart Structures and Systems*, 13(5), 821–848.

Salawu, O.S. (1997). "Detection of structural damage through changes in frequency: a review." *Engineering Structures.*, 19(9), 718–723.

Taguchi, G., and Jugulum, R. (2000). "New trends in multivariate diagnosis." *Indian J. Stat B*, 62: 233–248.

Tikhonov, A.N., and Arsenin, V.Y. (1977). *Solutions of Ill-posed problems*, New York, United States: Wiley.

Yang, Y.B., and Chang, K.C. (2009). "Extracting the bridge frequencies indirectly from a passing vehicle: Parametric study." *Engineering Structures*, 31(10), 2448–2459.

Yang, Y.B., Zhang, B., Qian, Y., and Wu, Y. (2018). " Contact-point response for modal identification of bridges by moving test vehicle." *International Journal of Structural Stability and Dynamics*, 18(5), 1850073.

Zhang, B., Zhao, H., Tan, C., O'Brien, E.J., Fitzgerald, P.C., and Kim, C.W. (2022). "Laboratory investigation on detecting bridge scour using the indirect measurement from a passing vehicle." *Remote Sensing*, 14 (13), 3106.